**PROBLEMY MECHATRONIKI**
**UZBROJENIE, LOTNICTWO, INŻYNIERIA BEZPIECZEŃSTWA**

**ISSN 2081-5891** **9, 3 (33), 2018, 57-74**

**PROBLEMS OF MECHATRONICS**
**ARMAMENT, AVIATION, SAFETY ENGINEERING**

# Heat Transfer Calculations in Barrel Cover of 35 mm Naval Armament System Gun

Andrzej DĘBSKI, Piotr KONIORCZYK, Zbigniew LECIEJEWSKI*, Marek PREISKORN, Zbigniew SURMA, Janusz ZMYWACZYK

*Military University of Technology, Faculty of Mechatronics and Aerospace, 2 Urbanowicza Str., 00-908 Warsaw, Poland*
* *Corresponding author's e-mail address: zbigniew.leciejewski@wat.edu.pl*

*Received by the editorial staff on 8 February 2018.*
*Reviewed and verified version received on 18 August 2018.*

DOI 10.5604/01.3001.0012.2739

**Abstract.** This paper presents the results of numerical simulations of non-stationary heat transfer in a 35 mm anti-air gun barrel cover made of composite materials. The cover protects the gun against weather conditions, including sea water effects, and serves as a protection against mechanical damage. It was assumed that heat coercion in this problem will be the heat condition reached by the material of the barrel with the cover removed, after firing three bursts of 7 shells each, 120 s after opening fire. It was assumed, that in the second 120, the gun crew installs the gun cover and at this point, the heating process begins, followed by cooling of the cover material. The problem of initial and boundary value in the barrel with a cover installed system was solved as a three-dimensional initial and boundary problem. The initial and boundary value model adopted for the coverless barrel and the calculation results for the first burst of seven shells was presented in paper [7]. To obtain the heat condition of the barrel in the second 120, it was necessary to perform calculations for the second and third bursts, and for the barrel cooling processes starting in the second 120.

The calculations were performed with a finite element method in the COSMOS/M software [9]. The cover material temperature values obtained during the numerical simulation are well below the temperature of 387K, which could form the upper limit of the composite applicability temperature range.
**Keywords:** mechanics, heat transfer, anti-aircraft gun barrel cover

## 1. INTRODUCTION

The anti-air defence of a ship or a group of ships can only be effective under modern-day naval warfare conditions if the technical resources making up the weapons system ensure sufficiently early detection and identification of targets posing the threat.

Trends in the development of modern naval anti-air artillery systems have been determined by the requirements of anti-missile and anti-aircraft defence. These require, for example: minimised dead zones, as short a reaction time as possible, high firing efficiency and as high effectiveness as possible at short ranges (within the dead zones of missile systems).

Qualitatively new requirements related to the achievement of objectives by the Polish Navy indicate a necessity of constant improvement of equipment related to performance of tasks intended to combat naval threats.

Therefore, since 2012, a scientific and industrial consortium (the Naval Academy in Gdynia, the Military University of Technology in Warsaw, PIT-RADWAR S.A. in Warsaw and ZM "Tarnów" S.A. in Tarnów) has conducted work on developing an entirely new Polish autonomous naval identification and artillery system capable of engaging air, sea and shore targets for the Polish Navy. A Polish 35 mm Naval Armament System, which is intended to constitute the armament of the minehunter Kormoran II, has been in trials since 2016 on the corvette ORP Kaszub. The system is characterised by being modular, scalable and having an open architecture. Its main components are:

1. 35 mm automatic naval gun system comprising, among others: cradle-mounted KDA 35 mm automatic gun (together with, among others, ammunition feed, firing, monitoring and control systems), gun control computer, inertial navigation system (INS), vertical and horizontal gun tracking system with stabilisation and limiters, data transmission system enabling communication with the Fire Control System (FCS), ALU control and diagnostics system, as well as protective cover against marine weather conditions (Fig. 1);
2. Integrated Tracking Unit (ITU) ZGS-158M comprising, among others: laser rangefinder, daylight camera, IR camera, IFF system, rotation and elevation drive system, ITU rotation and elevation control system with tracking line stabilisation, data transmission system, ALU control and diagnostics system. The ITU system is covered with a housing protecting against marine weather conditions (Fig. 2);

Fig. 1. 35 mm automatic naval gun installed on ORP Kaszub

Fig. 2. ZGS-158M unit on its mount

Fig. 3. Primary (left) and emergency (right) fire control stations

3. The fire control station (Fig. 3), equipped with a computer system and communication systems and enabling the management of the subordinate artillery system, will include two components:
   a) a primary fire control station, which includes: FCS with a fire control computer, gun, ITU, power supply and communication control consoles; vision visualisation terminal with subsystem status indication and a screen at the ship command station for viewing FCS visualisation,

b) an emergency fire control system, which includes: pedestal with ring sights, voice communication system with a basic fire control station, lead and elevation angle indicators, and control wheel with an electric trigger button.

The development process of the original Polish 35 mm Naval Armament System was an inspiration for solving numerous scientific problems, related to, for example, testing the effectiveness of original algorithms implemented in the FCS [1, 2, 3], intermediate period ballistics during a shot from the 35 mm barrel [4, 5], testing of gun and ITU stabilisation systems on a Stewart platform under simulated marine conditions [6] and barrel heat loading of the 35 mm gun [7], where results of numerical simulations of non-stationary heat transfer in the 35 mm gun barrel wall for a single shot and for a sequence of seven shots.

Continuing the deliberations begun in [7], this study analyses the issue of non-stationary heat transfer in the 35 mm gun barrel cover made of composite materials. The cover protects the gun against weather conditions, including sea water effects, and serves as a protection against mechanical damage. Because the barrel is air-cooled, the barrel cover can only be installed after the assigned fire mission is completed. A view of a gun section with barrel cover installed is shown in Figure 4.

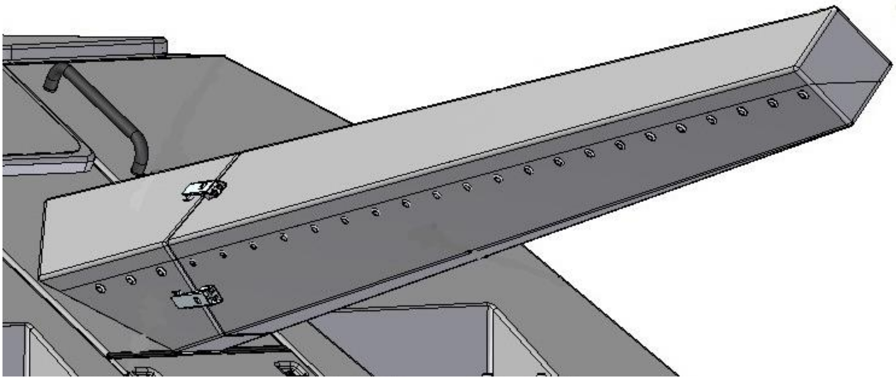

Fig. 4. View of gun section with barrel cover installed

It was assumed that:

– heat coercion in this problem will be the heat condition reached by the material of the barrel with the cover removed, after firing three bursts of 7 shells each,

– a single burst of 7 shots with the pause recommended by the manufacturer takes 5 seconds (0.7 s burst of 7 shots and 4.3 s pause); afterwards, another burst of 7 shots can be fired;
– at the 120th second from opening fire, the gun crew installs the gun cover and at this point, the heating process, followed by cooling of the cover material, is observed.

The calculation problem of a non-stationary temperature field in the barrel was solved as a two-dimensional, axially symmetrical initial and boundary value problem, isolating the profiles numbered 1 to 6 for calculation purposes Figure 5 [7].

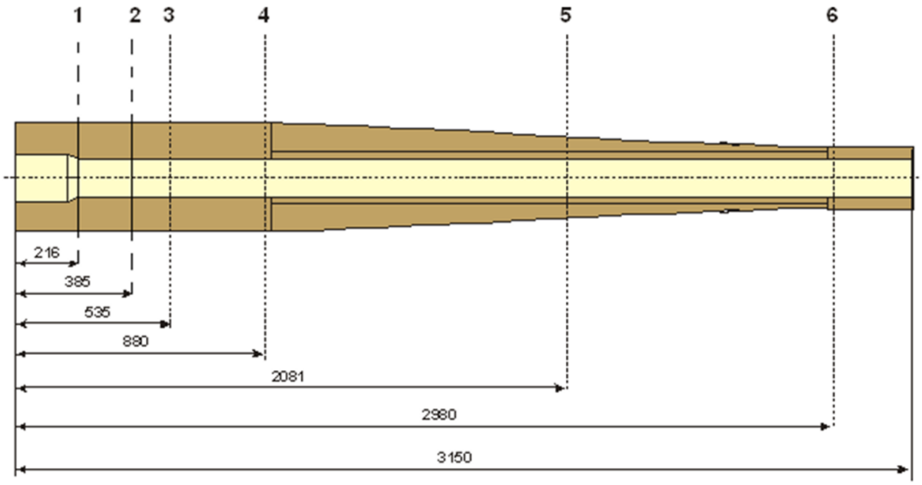


Fig. 5. Longitudinal profile of the gun barrel with indicated calculation profiles and external radii $r_z$ of the barrel wall.
S1: 0÷385 mm, $r_z$ = 55.0÷55.0 mm; S2: 385÷535 mm, $r_z$ = 55.0÷57.0 mm;
S3: 535÷880 mm, $r_z$ = 57.0÷59.5 mm; S4: 880÷2081 mm, $r_z$ = 59.5÷44.07 mm;
S5: 2081÷2980 mm, $r_z$ = 44.07÷31.0 mm; S6: 2980÷3150 mm, $r_z$ = 31.0÷31.0 mm

Sample results for temperature changes on the internal and external barrel surfaces for the most heavily loaded profile P6 (near the muzzle) for the third burst and cooling process, starting from time $t$ = 10 s to 20 s, are shown in Figure 6.

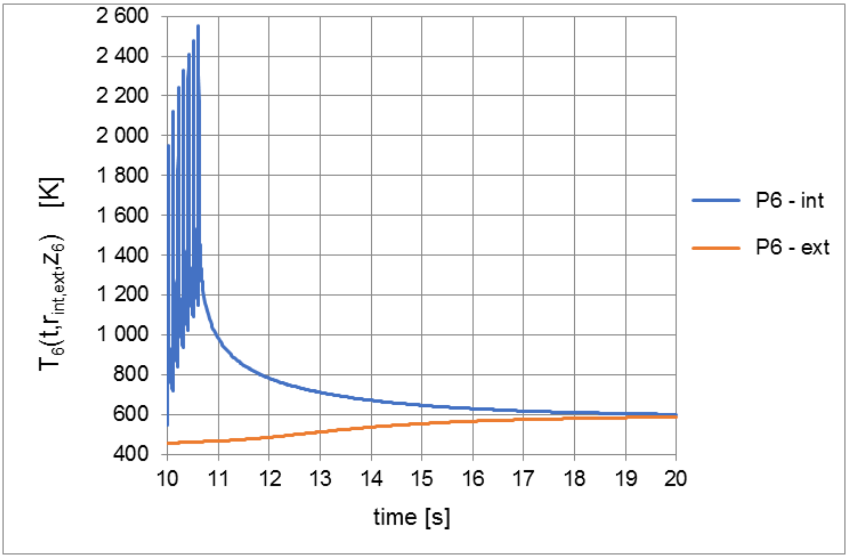


Fig. 6. Temperature changes on the internal (blue) and external (brown) barrel surfaces for the most heavily loaded profile P6 after the third seven-shot burst

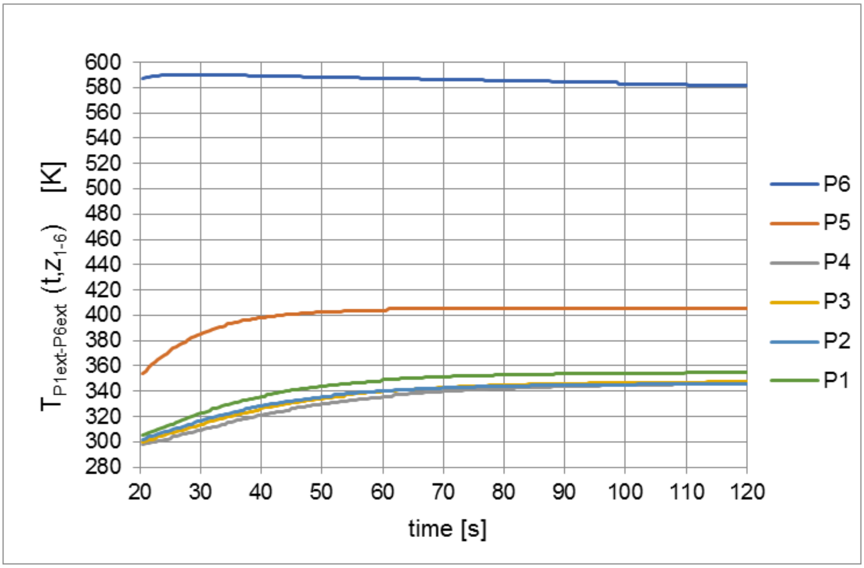


Fig. 7. Temperature changes on the external barrel surface at subsequent profiles from P1 to P6, during the period from time 20 s to 120 s

Sample charts of temperature changes on the external barrel surface as a function of time, within the range from $t$ = 20 s to 120 s, at subsequent profiles from P1 to P6, are shown in Figure 7.

The barrel cover is shorter than the entire gun and ends at profile P3, as the further part of the gun is inside the gun body. The problem of initial and boundary value in the barrel with cover installed system was solved as a three-dimensional initial and boundary problem. The barrel and cover structure has a vertical symmetry plane, marked with the letter A in Figure 8.

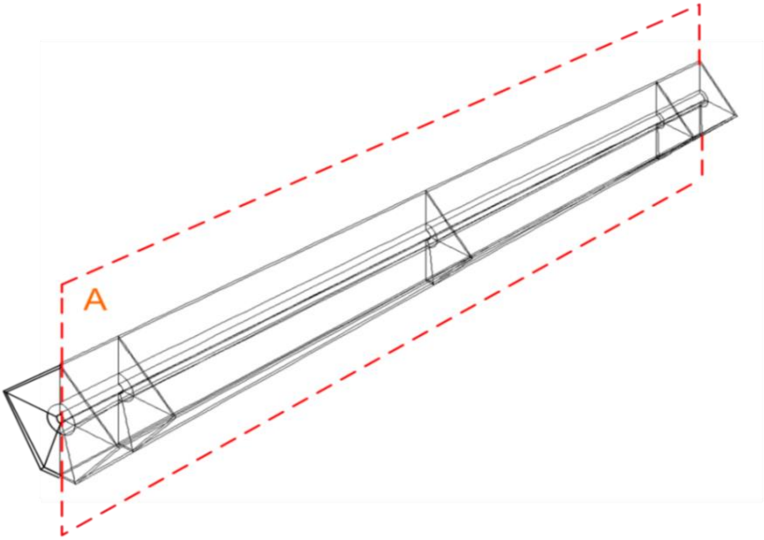


Fig. 8. Division of the entire barrel-cover assembly volume into two parts with a vertical symmetry plane running along the barrel axis

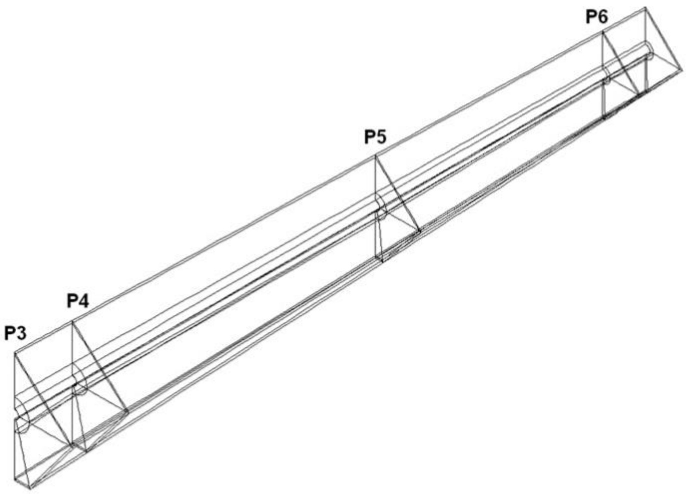


Fig. 9. Profiles P3-P6 of the barrel-cover assembly, adopted for the initial condition problem and the boundary conditions

It was assumed that the boundary conditions of initial and boundary value take values symmetrical in relation to plane A. Thus, the problem under consideration can be assumed as being symmetrical in relation to plane A, and the calculation area can be limited to a single half of the barrel-cover assembly. Figures 9 and 10 show the calculation area of the barrel-cover assembly model, with numbers of the initial condition problem zones for the barrel.

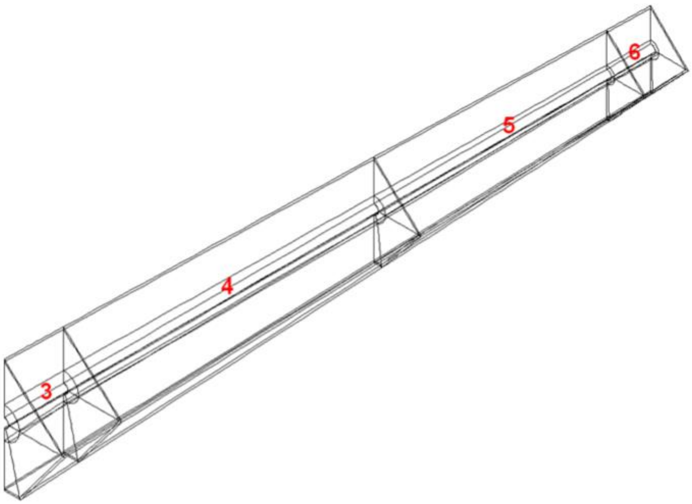


Fig. 10. Zones 3-6 of the barrel-cover assembly, adopted for the initial condition problem and the boundary conditions

## 2. THE INITIAL AND BOUNDARY VALUE PROBLEM

In this paper, the results of the non-stationary heat transfer equation with an initial condition and boundary condition for the barrel with a barrel cover are presented. It was assumed that during the barrel cooling process, no initial and boundary value occurs inside the barrel, i.e. heat flux density in the barrel $\dot{q} = 0$.

The initial and boundary value model also assumes that in the plane of profile P3 $\dot{q} = 0$. The four isolated zones of the barrel-cover assembly model, numbered 3 to 6, are shown in Figure 10. Initial barrel temperature values, equal for the entire zone, were defined based on the calculated temperature values for time $t$ = 120 s, averaged within the zone volume. The numeric values are provided in Table 1.

For the other parts of the model, an identical initial condition (IC) was assumed, i.e. temperature $T_0$ = 293 K. On the external surface of the cover, convective heat transfer was assumed, i.e.

$$\dot{q} = -\alpha \cdot \left(T_{cov.\ surface} - T_0\right)$$

Table 1. Assumed temperature values in zones 3÷6 of the barrel material for time $t$ = 120 s

| $i$ – zone number | $T_i$, K |
|---|---|
| 3 | 367 |
| 4 | 393 |
| 5 | 506 |
| 6 | 598 |

A substitute heat transfer coefficient value of $\alpha$ = 9.2 W/(m$^2$·K) was assumed, identical along the entire length of the barrel cover's external surface. An identical heat transfer coefficient value was assumed as for calculations of heat transfer in a barrel without the cover [7]. The barrel and barrel cover are separated by air in layers of thickness ranging from 10 mm to 30 mm. Based on the authors' own tests of thermal conductivity of unventilated air layers, the heat transfer value of the air layer between the external barrel surface and internal barrel cover surface was assumed at $\lambda$ = 0.2 W/(m·K), identical in all zones along the length of the cover [8]. At the muzzle, i.e. at the front of the barrel, it was assumed that the cover does not shield the muzzle (in reality, a cap that programs shells as they leave the barrel will be installed on the muzzle). For this surface, two boundary condition (BC) cases were analysed:

1. adiabatic condition of heat transfer, i.e. $\dot{q} = 0$;
2. convective heat transfer, i.e. $\dot{q} = -\alpha \cdot \left(T_{barrel\,surface} - T_0\right)$

As before, a substitute heat transfer coefficient $\alpha$ = 9.2 W/(m$^2$·K) and temperature $T_0$ = 293 K values were assumed. The gun barrel cover was made by the Plastwag S.A. company from Mielec (Poland), manufactured from composite boards varnished on one side. 6 mm thick boards contain resin and glass mat layers.

The authors of this paper measured the thermophysical properties of the composite, i.e. thermal conductivity, thermal diffusivity and specific heat at room temperature using an Applied Precision Isomet 2104 (Slovakia) device and test samples in the form of sections of varnished boards (Fig. 11). Ultimately, the following constant values of thermophysical properties of the barrel cover composite material were adopted for calculations:

– thermal conductivity $\lambda$ = 0.232 W/(m·K);
– specific heat $c_p$ = 982 J/(kg·K);
– composite density $\rho$ = 1660 kg/m$^3$.

Fig. 11. Test station for testing thermophysical properties of the gun barrel cover composite material using the Isomet 2104 instrument and the API 210412 surface probe (at room temperature)

## 3. NUMERICAL SIMULATIONS OF HEAT TRANSFER IN THE BARREL COVER

Numerical simulations of non-stationary heat transfer during the process of cooling the 35 mm gun barrel-barrel cover system were conducted. Temperature field distributions in the barrel cover and temperature changes as a function of time for the range of $t$ = 0 s (from the 120th second from opening fire, assumed the moment the cover is placed on the barrel) to $t$ = 3600 s were determined. Calculations were performed using the finite element method and the COSMOS/M software [9]. A grid of 8385 volumetric elements (prisms) and 13536 nodes was used.

Calculation results are presented as contour lines for selected profiles of the barrel-barrel cover assembly and on the external barrel cover surface at selected times, specifically for $t$ = 60 s, $t$ = 600 s, $t$ = 1800 s and $t$ = 3600 s. Temperature change charts as functions of time for selected points of the model are shown. These points lie at the edge of the material, i.e. on the internal and external surface of the cover material. Positions of selected points belonging to profiles P5 and P6 are shown in Figures 12 and 13.

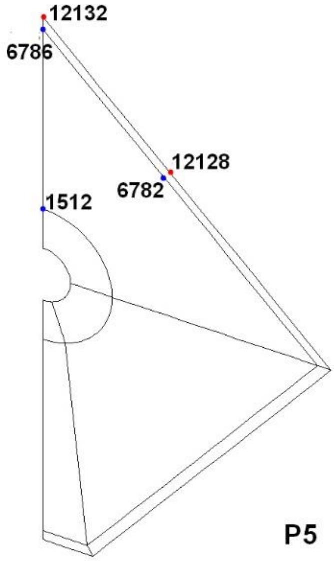


Fig. 12. Positions of points belonging to profile P5, for which temperature changes are shown as a function of time

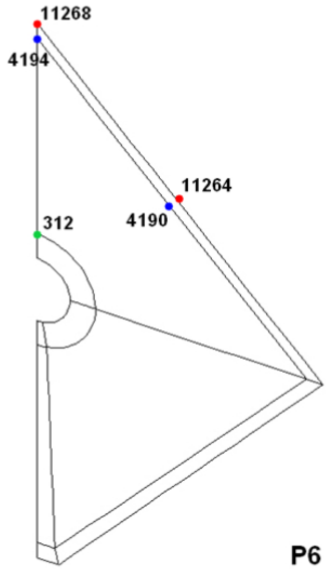


Fig. 13. Positions of points belonging to profile P6, for which temperature changes are shown as a function of time

Variant one: adiabatic heat transfer condition, i.e. $\dot{q} = 0$ on the front surface of the barrel;

Figures 14-18 show calculation results for the adiabatic BC on the front surface of the barrel at selected times $t$ = 60 s, 600 s, 1800 s, 3600 s from installing the cover.

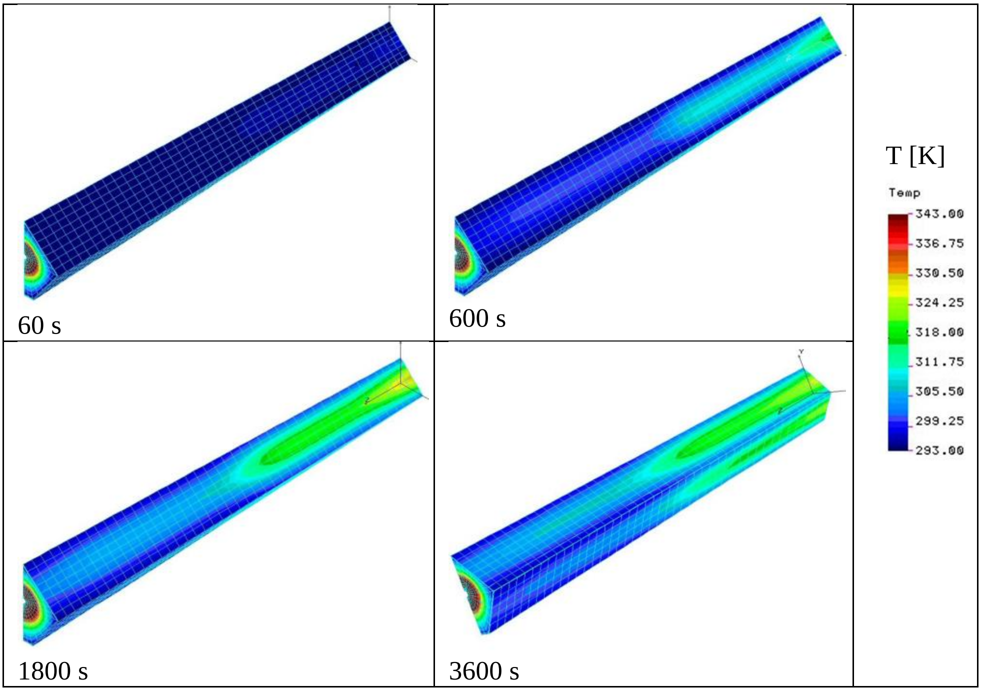


Fig. 14. Temperature field distribution on the external surface of the barrel cover at times $t$ = 60 s, 600 s, 1800 s, 3600 s from installing the cover. For time $t$ = 3600 s, a temperature distribution on the bottom surface of the cover is also shown

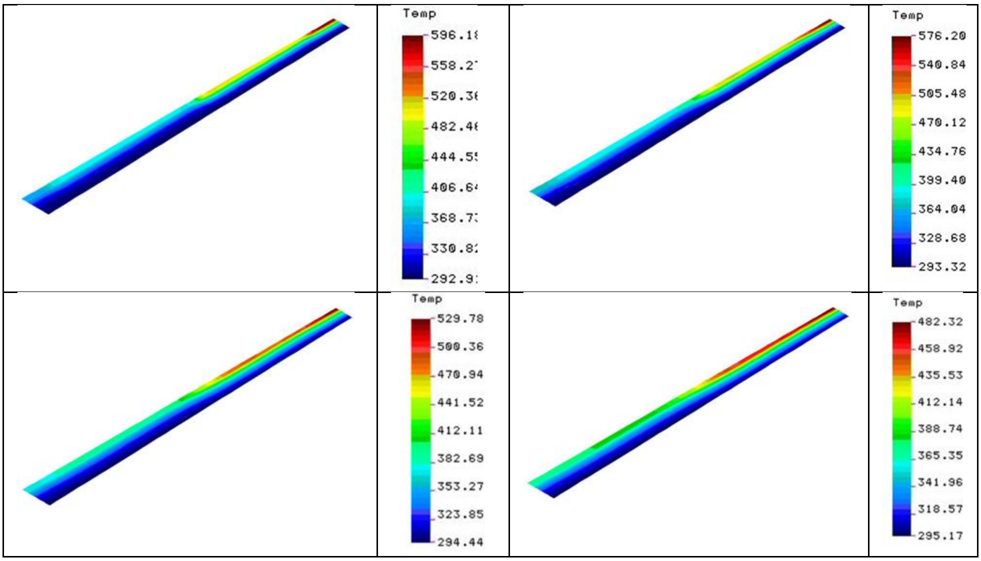


Fig. 15. Temperature field distributions in the horizontal profile of the barrel-barrel cover assembly at times $t$ = 60 s, 600 s, 1800 s, 3600 s from installing the cover (temperatures given in K)

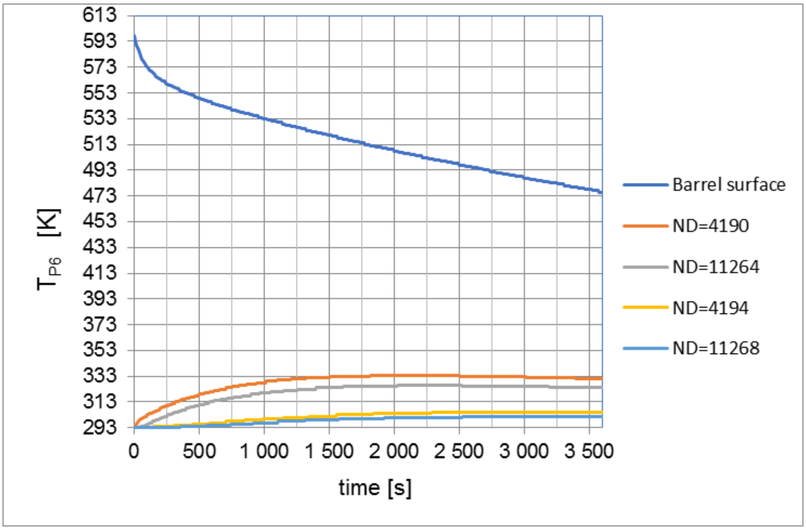


Fig. 16. Charts of temperature changes as a function of time in selected points of the cover in profile P6

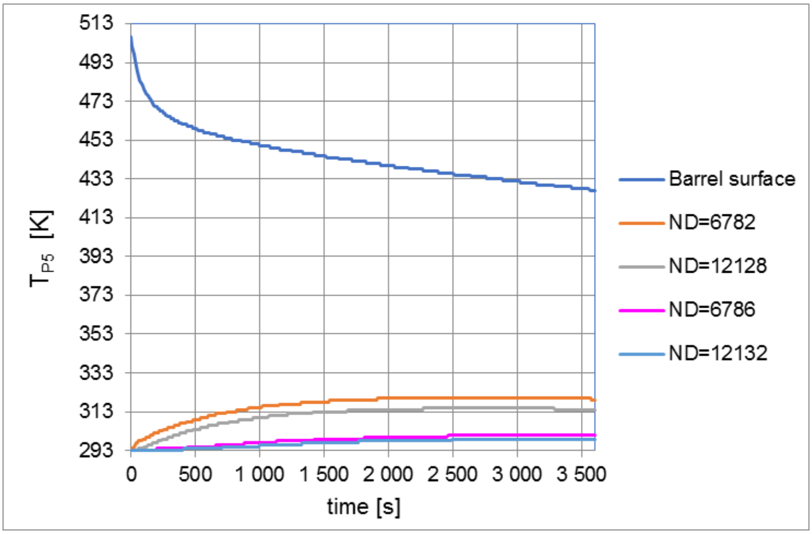


Fig. 17. Charts of temperature changes as a function of time in selected points of the cover in profile P5

Variant two: convective heat exchange on the front surface of the barrel was assumed, i.e. $\dot{q} = -\alpha \cdot \left(T_{barrel\ surface} - T_0\right)$.

The other boundary conditions and initial conditions remain unchanged.

Figure 18 shows temperature field distributions obtained in this variant on the external surface of the cover at times $t$ = 60 s, 600 s, 1800 s, 3600 s from installing the cover on the gun barrel.

Charts of temperature changes were calculated as a function of time in selected points of the cover in profiles P1-P6. Sample results – charts – for profile P6, where the highest temperature values occurred, are shown in Fig. 19.

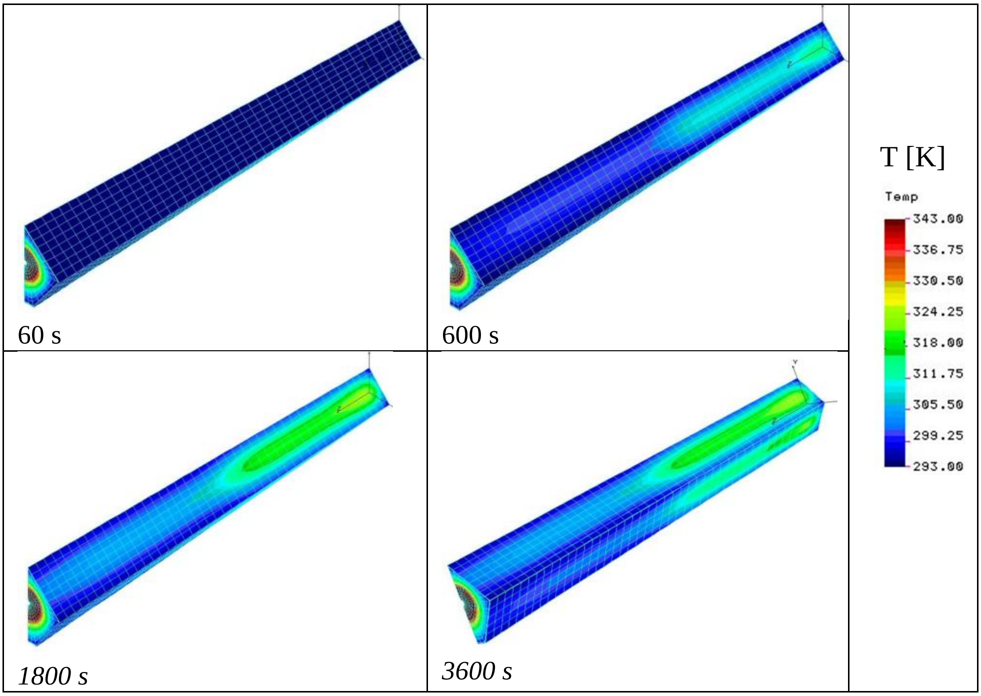


Fig. 18. Temperature field distribution on the external surface of the barrel cover at times $t$ = 60 s, 600 s, 1800 s, 3600 s from installing the cover (second variant of boundary conditions). For time $t$ = 3600 s, a temperature distribution on the bottom surface of the cover is also shown

Isothermal lines of temperature fields on external surfaces of the cover are similar for both calculation variants. Analysis of temperature changes as a function of time in selected points of profiles P1-P6 of the cover reveals that both the shape of temperature change charts as a function of time and the amplitude of cover surface temperature growth are virtually the same for both calculation variants. For the second boundary condition variant, a marked drop in temperature value by approx. 2-3 K occurs near the muzzle, compared to the first boundary condition variant.

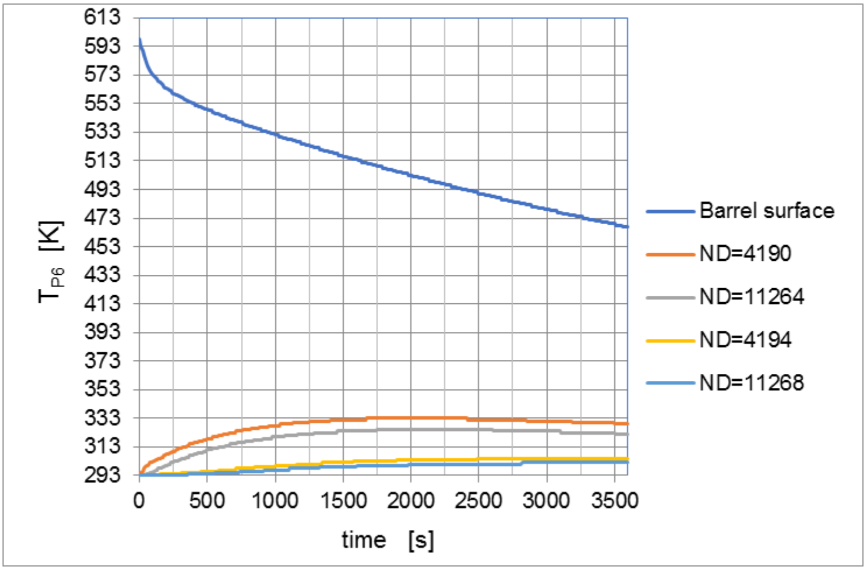


Fig. 19. Charts of temperature changes as a function of time in selected points of the cover in profile P6 for the second boundary condition variant

## 4. CONCLUSIONS

The results obtained for the heat transfer model assumptions used, concerning the heat condition of the barrel-barrel cover assembly at the time corresponding to cover installation (after firing three seven-shot bursts), show that internal cover surface temperature reached a maximum value of 338 K (65°C). The cover is going to reach this temperature after 1200÷1300 s from installing the cover. During the rest of the heat transfer process, the cover surface temperature lowers.

The authors' own tests conducted to determine the temperature characteristics of thermophysical properties of the cover material [10], performed using the NETZSCH DMA apparatus, revealed that in the proximity of the temperature of 387 K, the process of composite degradation begins. The cover material temperature values obtained during the numerical simulation are well below this temperature, which could form the upper limit of the composite applicability temperature range.

Following an experimental verification of the theoretical calculation results, a detailed heat transfer model will serve as a basis for studying the conditions and determining the criterion of installing the barrel cover after a specific firing cycle during the system's combat operation under naval conditions. The starting point for such analyses can be the land-based gun firing cycle shown in Fig. 20 [11].

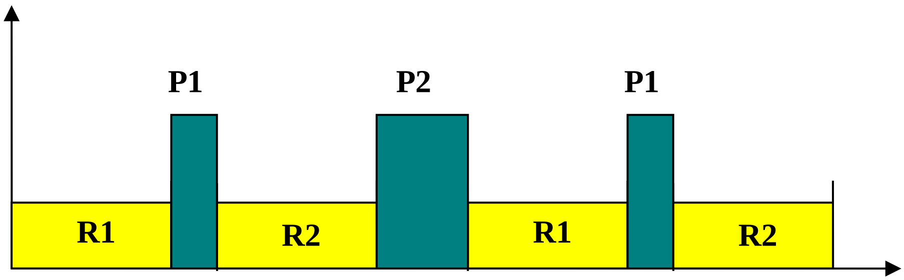


Fig. 20. Firing cycle for standard munitions and kinetic energy penetrators:
R1 – rhythm 1, R2 – rhythm 2; P1 – pause 180 seconds; P2 – pause 600 seconds

The term rhythm R1 is defined as firing 42 shows in the following sequence of events: three 7-shot bursts – 20 second pause – three 7-shot bursts, while rhythm R2 (firing 48 shots) is characterised by the following sequence: three 8-shot bursts – 20 second pause – three 8-shot bursts.

*The paper contains the results of the research work co-financed by the Polish National Centre for Research and Development 2012-2018 Scientific Fund, Project no. O ROB 0046 03 001*

## REFERENCES

[1] Kowalczuk Przemysław. 2014. *Metoda rozpoznawania obiektów trójwymiarowych dla potrzeb systemów kierowania ogniem*, rozprawa doktorska. Warszawa: Wydawnictwo Wojskowej Akademii Technicznej.

[2] Leciejewski Zbigniew, Tomasz Zawada, Przemysław Kowalczuk, Jacek Szymonik, Przemysław Czyronis. 2014. Selected Ballistic Aspects of Fire Control System Designed to Anti-Aircraft Gun. In *Proceedings of the 28th International Symposium on Ballistics*, 655-665. Atlanta, USA, 22-26.09.2014.

[3] Baranowski Leszek, Błażej Gadomski, Przemysław Majewski, Jacek Szymonik. 2016. "Explicit <<ballistic M-model>>: a refinement of the implicit "modified point mass trajectory model"". *Bulletin of The Polish Academy of Sciences. Technical Sciences* 64 (1) : 81-89.

[4] Czyżewska Marta, Radosław Trębiński. 2014. Modeling of Intermediate Ballistics of Modernized 35 mm Caliber Naval Gun. In *Proceedings of the 28th International Symposium on Ballistics*, 834-838. Atlanta, USA, 22-26.09.2014.

[5] Czyżewska Marta, Radosław Trębiński. 2015. „Wpływ urządzenia wylotowego lufy na przyrost prędkości pocisku w okresie balistyki przejściowej". *Problemy Mechatroniki. Uzbrojenie, lotnictwo, inżynieria bezpieczeństwa – Problems of Mechatronics. Armament, Aviation, Safety Engineering* 6 (2) : 87-98.

[6] Leciejewski Zbigniew, Sławomir Łuszczak. 2016. Stewart Platform as a Tool to Study the Stabilization of Aiming Line of Cannon and Line of Sight of Tracking Head. In *Proceedings of the 29th International Symposium on Ballistics*, 209-215. Edinburgh, Scotland, 9-13.05.2016.

[7] Dębski Andrzej, Piotr Koniorczyk, Zbigniew Leciejewski, Marek Preiskorn, Zbigniew Surma, Janusz Zmywaczyk. 2016. "Analysis of Heat Transfer in a 35 mm Barrel of an Anti-Aircraft Cannon". *Problemy Mechatroniki. Uzbrojenie, lotnictwo, inżynieria bezpieczeństwa – Problems of Mechatronics. Armament, Aviation, Safety Engineering* 7 (3) : 71-86.

[8] Koniorczyk Piotr, Janusz Zmywaczyk. 2008. „Pomiary i obliczenia przewodności cieplnej niewentylowanych warstw powietrza". *Ciepłownictwo Ogrzewnictwo Wentylacja* 7-8.

[9] *CosmosM Users Guide – A complete finite element analysis system*, Structural Research & Analysis Corp., Los Angeles, 2001.

[10] Koniorczyk Piotr, Marek Preiskorn, Janusz Zmywaczyk. 2016. Pomiary właściwości termofizycznych materiału osłony lufy armaty kal. 35 mm. W *Sprawozdanie z realizacji podtematu pracy badawczej w projekcie nr O ROB 0046 03 001*. Warszawa: Instytut Techniki Uzbrojenia WML WAT.

[11] Torecki Stanisław, Zbigniew Leciejewski, Zbigniew Surma. 2011. „Obliczenia temperatury lufy zdalnie sterowanego systemu przeciwlotniczego kalibru 35 mm dla przyjętego cyklu strzelania". *Problemy Techniki Uzbrojenia* 118 : 129-138.

# Obliczenia wymiany ciepła w osłonie lufy 35 mm armaty Okrętowego Systemu Uzbrojenia

Zbigniew LECIEJEWSKI, Andrzej DĘBSKI, Piotr KONIORCZYK, Marek PREISKORN, Zbigniew SURMA, Janusz ZMYWACZYK

*Wojskowa Akademia Techniczna, Wydział Mechatroniki i Lotnictwa, ul. gen. Witolda Urbanowicza 2, 00-908 Warszawa*

**Streszczenie.** W pracy przedstawiono wyniki symulacji numerycznych nieustalonego przewodzenia ciepła w osłonie lufy armaty przeciwlotniczej kalibru 35 mm wykonanej z materiałów kompozytowych. Osłona zabezpiecza armatę przed wpływem czynników atmosferycznych, w tym wody morskiej oraz stanowi ochronę przed uszkodzeniami mechanicznymi. Założono, że wymuszeniem cieplnym w tym zagadnieniu będzie stan cieplny osiągnięty przez materiał lufy ze zdjętą osłoną, po oddaniu trzech serii po 7 strzałów w każdej, po upływie 120 s od rozpoczęcia strzelania. Założono, że w 120. sekundzie obsługa armaty zakłada osłonę lufy i od tej chwili następuje proces nagrzewania się, a następnie chłodzenia materiału osłony. Zagadnienie wymiany ciepła w układzie lufa z nałożoną osłoną rozwiązano jako trójwymiarowe zadanie początkowo-brzegowe. Przyjęty model wymiany ciepła dla lufy nieosłoniętej i wyniki obliczeń dla pierwszej serii siedmiu strzałów autorzy przedstawili w pracy [7]. Do otrzymania stanu cieplnego lufy w 120. sekundzie konieczne było przeprowadzenie obliczeń dla drugiej i trzeciej serii strzałów, a także procesy chłodzenia lufy do 120. sekundy.

Obliczenia wykonano metodą elementów skończonych za pomocą programu COSMOS/M [9]. Wartości temperatury materiału osłony uzyskane podczas symulacji numerycznej mieszczą się znacznie poniżej temperatury 387 K, mogącej stanowić górną granicę zakresu temperaturowego stosowalności kompozytu.

**Słowa kluczowe:** mechanika, wymiana ciepła, osłona lufy armaty przeciwlotniczej